eng

MDPI

Review

A Review on the Synthesis and Current and Prospective Applications of Zirconium and Titanium Phosphates

Zakariae Amghouz [1], José R. García [2] and Alaa Adawy [3,*]

[1] Department of Material Science and Metallurgical Engineering, University of Oviedo, 33203 Oviedo, Spain; amghouzzakariae@uniovi.es
[2] Department of Organic and Inorganic Chemistry, University of Oviedo—CINN, 33006 Oviedo, Spain; jrgm@uniovi.es
[3] Unit of Electron Microscopy and Nanotechnology, Institute for Scientific and Technological Resources (SCTs), University of Oviedo, 33006 Oviedo, Spain
* Correspondence: a.adawy@outlook.com or uo263127@uniovi.es

Abstract: Metal phosphates represent an important group of materials with established industrial applications that are still attracting special scientific interest, owing to their outstanding physical and chemical properties. In this review, we account on the different synthetic routes and applications of zirconium and titanium phosphates, with a special focus on their application in the medicinal field. While zirconium phosphate has been extensively studied and explored with several reported industrial and medicinal applications, especially for drug delivery applications, titanium phosphates have not yet attracted the deserved attention regarding their established applications. However, titanium phosphates have been the focus of several structural studies with their different polymorphic forms, varied chemical structures, and morphologies. These variations introduce titanium phosphates as a strong candidate for technological and, particularly, biomedical applications.

Keywords: zirconium phosphate; titanium phosphate; nanolayered phosphates; nanofibrous titanium phosphate; chemical synthesis; crystal structure; technological applications; drug delivery; biomedical applications

Citation: Amghouz, Z.; García, J.R.; Adawy, A. A Review on the Synthesis and Current and Prospective Applications of Zirconium and Titanium Phosphates. *Eng* **2022**, *3*, 161–174. https://doi.org/10.3390/eng3010013

Academic Editor: Antonio Gil Bravo

Received: 31 December 2021
Accepted: 8 March 2022
Published: 14 March 2022

1. Introduction

Two-dimensional compounds represent an extraordinary group of materials that could provide fascinating scientific applications. The term ***laminar composite or lamellar solid*** is often associated with the concept of ***intercalation***, owing to the ability of this type of layered structures to accommodate guest molecules in between their layers, creating supramolecular materials. These intercalated guest molecules can be released accordingly and, therefore, these stratified solids have been conventionally considered as repositories (containers) for different functioning chemicals. Accordingly, intercalated laminar composites have characteristics of a dual nature and dual functions from both the host layered structures and their intercalated guest compounds. Herein, we focus on two of these laminar composites: zirconium phosphates and titanium phosphates, extending our review to their other variants and their established and prospective applications.

2. Zirconium Phosphates

Since the 1950s, many studies have focused on lamellar solids, particularly their properties and prospective applications. Special attention has been given to the development of innovative synthetic approaches for their preparation, and subsequent implementation in applications for different technological fields [1]. In this context, a group of laminar tetravalent metal phosphates is worth mentioning, with zirconium phosphates as remarkable structures that have attracted intensive investigation interests [2–4]. The great appeal

of zirconium phosphates (hereafter abbreviated as ZrP) is mainly attributed to their robustness, the versatility of their crystalline structure, and the tunability of their crystallinity degree. In addition, the textural properties of ZrP particles can be controlled by modifying the synthetic conditions, or chemistry of their layers, generally by introducing functional groups on their surface. In fact, the scientific interest in ZrP goes back to the beginning of the 20th century, when the first trials of using soluble zirconium salts, e.g., $ZrOCl_2 \cdot 8H_2O$, in the elimination of phosphate ions in solution were reported [5–7]. Since the 1920s, the thermogravimetric determination of zirconium, as ZrP, has been one of the most widely used quantitative analysis methods [8].

Although the cation exchange properties of ZrP began to be studied in the 1950s, the crystalline zirconium bis(monohydrogen phosphate) monohydrate, α-$Zr(HPO_4)_2 \cdot H_2O$ (α-ZrP), was not synthesized until 1964 [9]. In 1968, the description of its laminar structure was reported [10], for which more precise data appeared in 1969 [11]. The structural refinement of α-ZrP was published in 1977 in two independent articles [12,13], making it possible to explain the behavior of the material as cation exchangers after determining the position of the hydrogen atoms in the crystalline phase. The α-ZrP consists of a single plane of metal atoms linked through monohydrogen phosphate groups, located alternatively above and below each plane. Each zirconium atom is coordinated with six oxygen atoms of six different phosphates, and each phosphate tetrahedron shares three of its four oxygen atoms with three zirconium atoms, while the fourth is linked to a hydrogen atom, constituting the most active site of the material. The packing of the layers generates six-sided cavities that contain the water molecules, which interact through hydrogen bonds with the P–OH groups in the same plane (Figure 1).

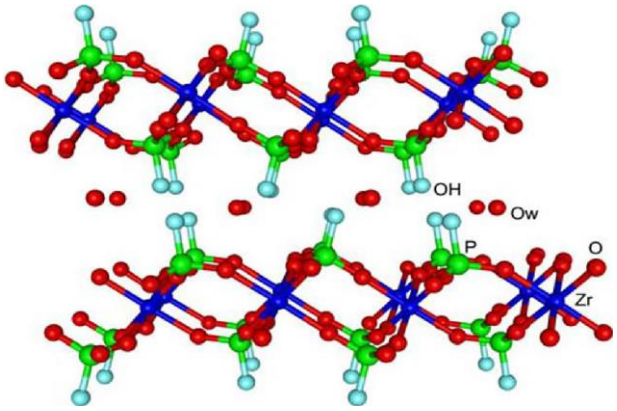

Figure 1. The crystalline structure of α-ZrP. Reprinted with permission from reference [14].

2.1. Reported Methods for α-ZrP Synthesis

Three main routes for the synthesis of crystalline α-ZrP have been described: (i) the reflux methods; (ii) the metal complexing reagent-utilizing methods; and (iii) the hydrothermal methods.

The reflux method was first published by Clearfield and Stynes in 1964 [9]. In this method, an amorphous solid is obtained from the direct reaction between phosphoric acid (H_3PO_4) and zirconyl chloride, ($[Zr_4(OH)_8(H_2O)_{16}]Cl_8(H_2O)_{12}$), that is subsequently washed with distilled water to eliminate all chloride ions, before being refluxed in concentrated phosphoric acid until obtaining crystalline α-ZrP. The degree of crystallinity varies directly with the refluxing duration and the concentration of the used phosphoric acid solutions. Worth noting that almost four decades later, it was demonstrated in our laboratories that the formation of amorphous zirconium phosphate is actually a consequence of washing the precipitate with distilled water [15]. This led to the conclusion that crystalline α-ZrP can be directly obtained after the reaction between acid phosphoric and zirconyl chloride at room temperature, although the obtained α-ZrP microcrystals easily hydrolyze in water [15].

On the other hand, the use of complexing agents for the synthesis of highly crystalline α-ZrP was first proposed in 1968 by Alberti and Torracca [16]. This approach, dubbed the HF method, includes the complexation of the Zr(IV) cation with fluoride anions, to form with ZrF_6^{2-} species, and its slow subsequent decomposition in the presence of phosphoric acid. The degree of α-ZrP crystallinity is controlled through the rate of HF elimination. García-Rosales et al. revisited this approach to study the precipitation of α-ZrP from solutions of fluoro complexes of zirconium (IV) using Mexican zirconium sand as raw material [17]. The oxalate anion ($C_2O_4^{2-}$) was also reported to be another complexing agent for zirconium (IV). Horsley et al. [18] and Capitani et al. [19] explored the synthesis of α-ZrP using oxalic acid (HO_2C-CO_2H). Their studies showed that the obtained material had similar structural characteristics and properties to those prepared in the presence of hydrofluoric acid (HF), with the additional advantage of providing more efficient reaction yields in shorter times.

As a third alternative, Shuai et al. proposed the use of a hydrothermal method based on the slow addition (under stirring) of a zirconyl chloride ($[Zr_4(OH)_8(H_2O)_{16}]Cl_8(H_2O)_{12}$) solution to phosphoric acid (H_3PO_4) solutions, followed by subsequent heating of the reaction mixture to 200 °C [20]. They observed that the length and thickness of the crystalline α-ZrP [$Zr(HPO_4)_2 \cdot H_2O$] plates are directly proportional to the concentration of phosphoric acid, whereas their length/thickness varies inversely. They also studied the growth rate of α-ZrP crystals as a function of reaction time and phosphoric acid concentration. They found that the process starts with a rapid homogeneous nucleation in the presence of an amorphous phase, in a regime similar to liquid–liquid phase separation that was first reported by Vekilov et al. as the very first step of nucleation [21]. This is followed by slow progress, especially at low concentrations of phosphoric acid. This slowness in the metastable stage allows for autoselection of better nuclei and the formation of secondary clusters, from which crystals grow with an observable homogeneity and regularity in size and morphology of the crystals, after dissolving poorly ordered crystals and their reprecipitation (Figure 2) [22]. This nucleation and crystallization mechanism resembles what was known later in the literature as the two-step nucleation mechanism that was mainly reported for protein crystallization, and very recently, for metal–organic frameworks [21,23,24].

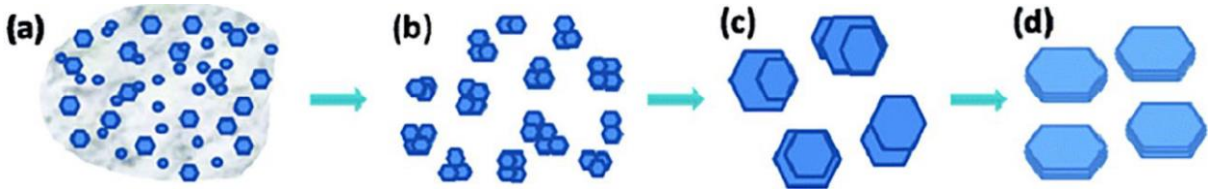

Figure 2. Representation of α-ZrP crystal formation. (**a**) Precipitation of nanocrystals and amorphous particles from solution. (**b**) Lattice orientation of nanocrystals with formation of secondary clusters. (**c**) Growth of microcrystals from secondary clusters. (**d**) Formation of homogeneous and regular crystals by dissolving poorly ordered areas and subsequent re-precipitation. Reprinted with permission from reference [20], License number: 1173274-1.

Later, Cheng et al. described the synthesis of α-ZrP, but rather in the form of rods, in addition to the usual morphology of plates, as a function of the presence or absence of small amounts of fluoride ions [25]. They showed that in the absence of fluoride ions, mixing zirconyl chloride and concentrated phosphoric acid solutions, that is followed by heating the mixture at 100–120 °C, resulted in the formation of plate-shaped α-ZrP, with a notable increase in crystallinity with increasing temperature. On the other hand, the presence of small amounts of fluoride ions led to the formation of rod-shaped α-ZrP together with the plate-shaped α-ZrP crystals. They attributed the growth of crystals along the crystallographic *a*-axis to be due to the selective adsorption of fluoride ions on the surface of the plates.

Other unconventional strategies for the synthesis of α-ZrP were reported to have resulted in the formation of microcrystals with different morphologies and textural properties. As an example, Benhamza et al. used a sol–gel synthesis in which a concentrated

phosphoric acid solution was added to zirconium (IV) propoxide [$Zr(OCH_2CH_2CH_3)_4$] in 1-propanol ($CH_3CH_2CH_2OH$) [26]. The aging in the mother liquor increased the degree of crystallinity of the resultant α-ZrP, which varied in structure from amorphous to semi-crystalline materials. Another approach was reported by Hajipour et al. who prepared hexagonal shaped α-ZrP nanoparticles using polyvinyl alcohol [$-CH_2CHOH-]_n$ (PVA) or polyvinylpyrrolidone [$(C_6H_9NO)_n$] (PVP) in an aqueous solution [27]. PVA and PVP acted as complexing organic matrices for Zr(IV) that facilitated the dispersion of α-ZrP particles and controlled their sizes. Afterwards, their (PVA/PVP) elimination through the calcination led to the growth of hexagonally-shaped plates with an average length of 60 nm.

On the other hand, mesoporous zirconium phosphate that bears relatively high specific surface areas and proton conduction capacity [28,29], are usually synthesized by calcination of the reaction product of soluble phosphate and/or phosphonate salts with zirconium oxychloride ($ZrOCl_2$) or zirconium alkoxide [$Zr(OR)_4$] [30–33]. Moreover, Zhao et al. used the reaction between phosphoric acid and zirconium propoxide, in the presence of non-ionic surfactants, to obtain gels that transformed to ZrP with a vermicular morphology after being thermally activated [34]. Furthermore, Tarafdar et al. synthesized spherical zirconium phosphate particles (micro- and meso-porous) with zirconium carbonate [$Zr(CO_3)_2$] as the source of the metal [35]. In addition to the above, Zhu et al. obtained α-ZrP with unusual textural properties, using an approach consisting of a sol–gel process followed by supercritical drying [36]. For this process, two polymers: polyethylene glycol [$H-(O-CH_2-CH_2)_n-OH$] (PEO) and polyacrylamide [$(-CH_2CHCONH_2-)$](PAM), were used that led to the formation of solids with macropores of controllable size (0.5–5 μm). These solids can be modified through altering the relative proportion of both polymers. These materials in monolithic form maintain high porosity, with specific surface areas close to 600 $m^2 \cdot g^{-1}$, and good mechanical properties in uniaxial compression.

2.2. Functionally-Adapted α-ZrP Synthesis Routes

The increasing interest in nanotechnology demands the development of new synthetic approaches for laminar materials as α-ZrP, in order to prepare nanoparticles of nanometric dimensions, both in their planes (length/width) as well as in their thickness, until reaching colloidal dispersions of quasi-individual sheets.

In that respective, Bellezza et al. proposed the synthesis of α-ZrP nanoparticles from water-in-oil microemulsions containing zirconyl chloride and phosphoric acid [37]. In addition, Alberti et al. synthesized α-ZrP of low crystallinity in a one-step reaction, where a solution of an organic zirconyl salt such as zirconyl propionate [$Zr(CH_3CH_2COO)_4$], in a polar aprotic solvent (e.g., *N*,*N*-dimethylformamide [$(CH_3)_2NC(O)H$], DMF) is mixed at room temperature with a solution of phosphoric acid in the same solvent, inducing the formation of a transparent dispersion from which the solvent is removed by heating to dryness [38]. Although this procedure is chemically effective, the use of organic solvents deprives it from being an ecologically friendly alternative and, thus, biocompatible for medical applications [39]. In order to develop synthetic procedures with less environmental drawbacks by avoiding the usage of toxic solvents, ethanol (C_2H_5OH) was used to dissolve zirconyl propionate [40]. This led to the formation of gel-like materials containing crystalline domains of α-ZrP sheets intercalated with ethanol. Heat treatment of these gels generates irregularly shaped α-ZrP nanoplates. As expected, the presence of low-coordination phosphate groups ($H_2PO_4^-$ and H_3PO_4) was detected in α-ZrP nanoparticles in a much higher proportion than in massive materials, which favors their reactivity compared to microcrystalline materials.

2.3. Technological Applications of α-ZrP and Their Introduction in Medicinal Chemistry

In addition to its well-known applications as ion exchangers that can assist in purification [41,42], and proton conductors [43,44], or catalysts and catalyst supports [14], α-ZrP and its derivatives have been explored to obtain different functionalities, such as anticorrosion coating and reinforced mechanical properties.

Owing to its barrier property, exfoliated α-ZrP, after being functionalized with polypyrrole, could be used for the fabrication of waterborne epoxy coatings (PPy-ZrP/WEC), that bear outstanding anticorrosion resistance [45]. In another context, despite the difficulty of introducing inorganic nanoparticles homogenously in a polymeric matrix, different amounts of bromine initiator could be introduced on the surface of α-ZrP nanoplatelets using a dual-epoxide-modified method [46] that facilitated their usage to graft polymethylmethacrylate (PMMA) polymer. This resulted in enforced mechanical properties for the resultant matrix (ZrP-g-PMMA) that could present a new alternative to this PMMA polymer, widely used for biomedical applications [47].

α-ZrP and its derivatives have also been extensively investigated in biomedical applications. The implementation of nanotechnology for drug delivery processes has become a very promising area of research, with a primary objective to realize the necessity to completely eliminate (or even inhibit) the inherent side effects for the compulsory administration of medications. In this context, lamellar zirconium phosphate can serve as a good choice for being a carrier material in drug delivery systems owing to its excellent biocompatibility [48–51]. This has allowed for its commercial use in peritoneal dialysis as a sequestrant of ammonium cations [52].

The intercalation capacity of α-ZrP facilitates the incorporation of functional biomolecules into its structure, avoiding their unnecessary interaction with the biological environment, preventing their protein denaturation, and prolonging their lifetime and thus, their biofunctionality. The acidic character of the interlaminar hydrogen phosphate groups favors the reversible intercalation of basic species and, therefore, the ability to sequester and release molecules of biological interest. In general, the expulsion of the molecules contained in the lamellar inorganic matrices is achieved by alterations in the chemical environment, such as a concentration gradient or changes in pH, and other biological stimuli [48–51].

Ding et al. were the first to intercalate proteins in microcrystalline α-ZrP [53]. Afterwards, Kumar and McLendon described the intercalation of heme proteins with redox activity [54]. Thereafter, Kim et al. obtained multilayer thin films comprising previously exfoliated α-ZrP sheets and polycations, such as cytochrome c (a monomeric protein that acts as a mitochondrial electronic transporter) [55]. In addition, α-ZrP was also used to immobilize myoglobin, lysozyme, hemoglobin, chymotrypsin, and glucose oxidase [56]. Furthermore, Bellezza et al. immobilized lipase on pristine and functionalized α-ZrP, observing that the amount of lipase retained increases as the hydrophobicity of the surface increases [57]. Moreover, it was observed that the presence of DNA or urea stabilizes the activity of enzymes and proteins in α-ZrP based nanomaterials. For example, the activity of hemoglobin inserted in α-ZrP is greater when it is co-intercalated with DNA [58], while moderate concentrations of urea stabilize heme proteins (methemoglobin and metmyoglobin) retained in α-ZrP, thus increasing its activity as well as its average lifetime by alterations in the chemical environment [59].

A quite different biologically relevant application is the one that has been reported by Xu et al., who selectively captured phosphopeptides in complex mixtures using α-ZrP nanoplates, in order to analyze tryptic digestions of mouse liver and leukemia cell phosphoproteomics, identifying 158 phosphopeptides (209 phosphorylation sites) of 101 phosphoproteins in mouse liver lysate, and 78 phosphopeptides (104 phosphorylation sites) of 59 phosphoproteins in leukemia cell extract [60]. On the other hand, Díaz et al. studied the controlled release of nanoencapsulated insulin in α-ZrP, using pH variations as a stimulus [48]. Afterwards, they reported the use of zirconium phosphate nanoplates for the encapsulation of cisplatin (a well-known drug in chemotherapy treatments against various types of cancer) and its administration to tumor cells [51]. Cisplatin, which was inserted using ion exchange, was tested in vitro for cytotoxicity against human breast cancer (MCF-7) with promising results. The intercalated drug was released only at low pHs, typical for tumor cells, which should minimize the side effects of cisplatin on noncancerous tissue. In addition, these researchers used α-ZrP to intercalate doxorubicin (DOX), a cytostatic from the anthracycline family, widely used in cancer chemotherapy, demonstrating its

effectiveness against MCF-7 cells compared to free DOX, in a process that leads to the uptake of nanoparticles by endocytosis, reaching and penetrating cancer cells to a greater extent than healthy cells [50]. In this mechanism, the hydrogen-mediated phospholipid cell membrane phosphates participate with P-OH groups on the surface of α-ZrP. Studies by others on DOX@α-ZrP demonstrated that the zirconium phosphate nanoparticles are highly hemocompatible and do not show hemolytic activity towards human red blood cells [49]. González et al. conducted in vitro studies showing that α-ZrP nanoplates deliver DOX to cancer cells, while DOX retains its original anticancer activity [61]. Furthermore, while DOX induces the generation of oxygen radicals in both cancer cells and healthy mammary epithelial cells, DOX@α-ZrP causes greater oxidative stress in MCF-7 breast cancer cells than in MCF-10A breast epithelial cells, thus showing selective toxicity towards cancer cells. Subsequent studies have reported the success of modifying the surface of the zirconium phosphate in DOX@α-ZrP, improving the ability to administer DOX, and increasing its biocompatibility [62].

Another variety of α-ZrP (3-aminopropyl)triethoxysilane [$H_2N(CH_2)_3Si(OCH_2CH_3)_3$] (APTES) functionalized zirconium phosphate nanoparticles has also been used for drug delivery. Li et al. used APTES@α-ZrP to anchor hyaluronic acid (HA) to combine the carrying capacity of the drug in zirconium phosphate and the tumor targeting capacity of HA in the administration of paclitaxel (PTX), a drug used in the treatment for cancers of the lung, ovary, breast, and advanced forms of Kaposi's sarcoma [63]. In vivo experiments in A549 lung cancer showed good antineoplastic ability and minimization of the toxic side effects of PTX.

Donnadio et al. prepared materials with antimicrobial and antibiofilm activity using nanocrystalline α-ZrP as a carrier for chlorhexidine (CLX), which was used to prepare carboxymethylcellulose (CMC)-based composite polymeric films as wound dressings with reduced cytotoxicity, in order to release the antiseptics in a prolonged way, showing good antibacterial activity against Gram-positive and Gram-negative bacteria [64]. CMC@α-ZrP films are uncytotoxic to human dermal fibroblast and keratinocyte cell lines. When CLX was incorporated into CMC@α-ZrP, its cytotoxicity was significantly reduced when compared to free CLX, probably because of the controlled release of CLX that kept its concentration at low levels.

Very recently, Adawy et al. implemented the hydrothermal methodology to synthesize monohydrated nanolaminar α-ZrP and subsequently enriched their nanolayers with silver nanoparticles (AgNPs) of uniform dimensions and distribution [65]. The structural stability of α-ZrP was confirmed before and after enrichment with AgNPs as well as the assessment of their antimicrobial activity and the cytocompatibility. They reported that the pristine α-ZrP did not show any cytotoxic effects against Sarcoma osteogenic cells, with a small loss of its biocompatibility when enriched with silver, yet with outstanding antimicrobial effectiveness against *Escherichia coli*.

3. Titanium Phosphates

Although zirconium phosphates have so far been the most studied lamellar solids of all tetravalent metal phosphates since 1950s, titanium laminar phosphates have also attracted particular attention around a decade later (1960s). Alberti et al. [16,66], following the wake of the seminal investigations on zirconium phosphates by Clearfield et al. [9], were pioneers in the study of crystalline titanium phosphates. In addition, the contributions of the Soviet school are also noteworthy in this field, with special mention to Chernorukov et al. [67]. In this scientific environment, our working group at the University of Oviedo (Research Group of Synthesis, Structure and Technological Application of Materials [SYSTAM], https://systam.grupos.uniovi.es/) published its first articles on titanium phosphates in the early 1980s [68–70]. The established synthetic routes for the layered titanium phosphate [α-Ti $(HPO_4)_2 \cdot H_2O$] are very similar to those of layered zirconium phosphate [α-$Zr(HPO_4)_2 \cdot H_2O$]. Only recently new methodologies have been introduced, mostly based on the hydrothermal synthesis, but rather using other compounds as precursors, such as protonated layered lepidocrocite-type $K_{0.7}(Ti)_2O_4$ [71]. Unlike zirconium

phosphates, titanium phosphates can be also synthesized in another morphology, exhibiting the form of nanorods, and thus are known as nanofibrous titanium phosphates. The most popular synthetic route of nanofibrous titanium phosphates is also the hydrothermal method at temperatures 160–250 °C, using a titanium precursor such as titanium tetrachloride ($TiCl_4$) in aqueous phosphoric acid solutions [72]. Moreover, several studies have reported on the possibility for growing a nanofibrous titanium phosphate thin film on titanium substrates after hydrothermally treating the latter in phosphoric acid solutions at 180 °C [73] or 250 °C [74], but also at 120 °C in the presence of hydrogen peroxide as a catalyst [75]. Herein, we provide further details on the different titanium phosphate phases, categorizing them into nanolayered and nanofibrous phases.

3.1. Nanolayered Titanium Phosphates

So far, there are three nanolayered titanium phosphates reported in the literature. The crystalline titanium bis(monohydrogen phosphate) monohydrate, α-Ti $(HPO_4)_2 \cdot H_2O$ (α-TiP), is an iso-structure of its zirconium counterpart (α-ZrP) [76]. γ-titanium phosphate (γ-TiP), formulated as γ-$Ti(HPO_4)_2 \cdot 2H_2O$ and later as γ-$Ti(PO_4)(H_2PO_4) \cdot 2H_2O$, is another interesting dihydrate layered material that is considered as an analogue to α-TiP, with larger interlayer spacing than α-TiP since it comprises two interlayer water molecules. γ titanium phosphate (γ-TiP) is also an iso-structure of γ zirconium phosphate, so do its dehydrated form known as β-TiP [β-$Ti(PO_4)(H_2PO_4)$] and β-ZrP [β-$Zr(PO_4)(H_2PO_4)$] [77–79]. As expected, α-TiP and γ-TiP have many profound applications, such as ion exchange [80], catalysis [30], ionic conductivity [44,81], and electrodes for Li- and Na ion storage [82–84], in addition to their capability of being functionalized with organic species and also being exfoliated [85–87]. Nevertheless, there is almost no record for their biologically relevant applications.

3.2. Nanofibrous Titanium Phosphates

Several titanium phosphate compounds have been reported with different morphologies and thus different plausible applications [88–91]. With a nanofibrous morphology, two polymorphs with the chemical formula: $Ti_2O(PO_4)_2 \cdot 2H_2O$, called π-TiP and ρ-TiP, were synthesized around two decades ago [72]. Although π-TiP and ρ-TiP are compounds with neutral lattices, they exhibit an outstanding ability to incorporate intracrystalline metal cations through ion exchange processes [92,93]. Particularly, π-TiP reaction with alkali metal nitrates in the molten state results in the formation of fibrous phases charged with the reactant alkali metal [92]. In terms of their crystallographic structures, the structure of ρ-TiP was reported shortly after being solved ab initio from synchrotron X-ray and neutron powder diffraction data (Figure 3a) [94]. On the other hand, there were only some scientific hypotheses reported about the most probable structural ordering of π-TiP [92]. The crystal structure of the ρ-TiP phase has two channels that run parallel to the crystallographic *a*-axis in which the water molecules are housed. Recently, we succeeded to reveal the crystal structure of π-TiP [95]. The π-TiP phase, obtained under mild hydrothermal conditions, crystallizes in the monoclinic system (space group $P2_1/c$) in contrast to the previously described ρ-TiP (triclinic, *P*-1). The π-TiP structure is made up of TiO_6 and $TiO_4(H_2O)_2$ octahedra, connected with orthophosphate groups, defining the anisotropic three-dimensional packing, consistent with the existence of preferential crystal growth directions. The properties of both polymorphs have scarcely been explored, probably because they were just synthesized less than 3 decades ago. Although both π- and ρ-TiP exhibit low accessible porosity when hydrated (11–16 $m^2 \cdot g^{-1}$) [96], Amghouz et al. showed that this can be changed significantly if they are treated thermally. In such a process, the crystallized water molecules are eliminated, and the resultant dehydrated phases exhibit an unusual adsorption capacity for nitrogen a little above ambient temperature [97]. For the ρ-TiP, the thermal treatment at temperatures of 200–300 °C results in the generation of tetrahedral (ex-octahedral) titanium atoms (Figure 3b) that are responsible for the enhanced nitrogen adsorption capability [97]. On the other hand, this treatment for the π-TiP was shown to lead to a change in the coordination environment of one of the titanium atoms, which

goes from octahedral to tetrahedral, with the formation of the anhydrous $Ti_2O(PO_4)_2$ [97]. Beside their nitrogen adsorption properties, π-TiP has been recently investigated for its proton conductivity. π-TiP was doped in a chitosan matrix to study the proton conductivity of the resultant chitosan-based composite membranes (CS@π-TiP) [95]. This study showed that doping the CS matrix with π-TiP (5 w/w%) results in a 1.8-fold rise in the proton conductivity compared to the bare membrane [95]. Another explored property is their attraction to water. Yada et al. prepared super-hydrophilic thin films made up of micro- and nano-crystals of π-TiP with controlled morphologies that transform to superhydrophobic layers when π-TiP is modified with alkylamines [75]. Similarly, Cai et al. showed that TiP thin films grown on titanium substrates can possess a hydrophilicity that can be switched to a super-hydrophobicity through increasing the preparation temperature [98]. Recently, π-TiP has been reported to possess ultrastability as a Ca^{2+} storage material with a minimal dimensional change and almost no transformation in the crystallographic structure upon the insertion or extraction of Ca^{2+} [99]. This exceptional stability that stands for over 1700 cycles of the Ca^{2+} insertion and extraction presents π-TiP as a viable electrode material for calcium-ion battery applications [99]. Therefore, we can estimate that many attempts could be made in the near future to utilize these nanofibrous phases for some of the other applications that have been established for the nanolayered titanium phosphates.

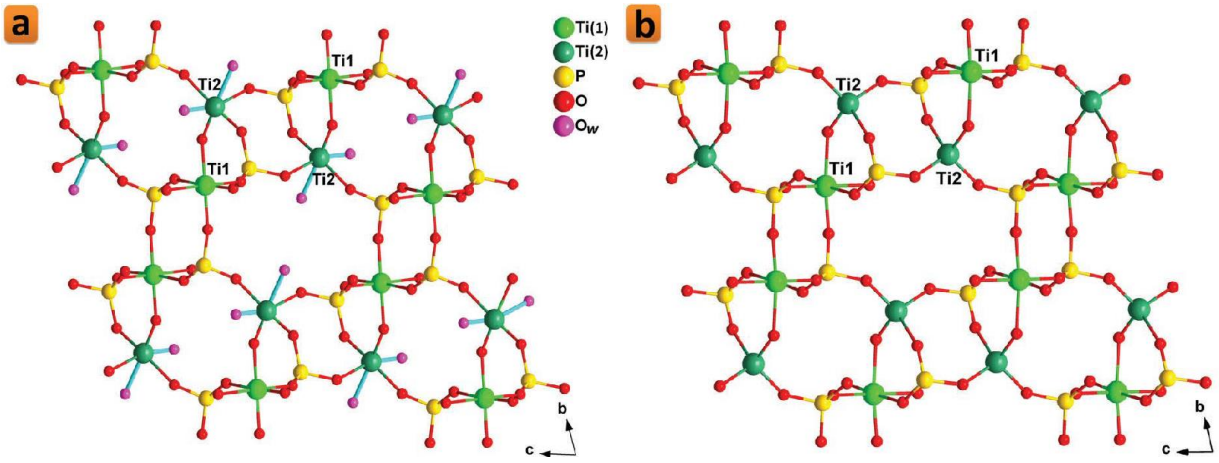

Figure 3. Crystalline structure of the dihydrate (**a**) and anhydrous (**b**) phases of ρ-TiP. Reprinted with permission from reference [86], License number: 1173277-1.

3.3. Prospective Applications of TiP in the Biomaterials Research Field

Since α-TiP is an iso-structure of α-ZrP, and has been reported to share many of its physical and chemical properties beside its non-spherical layered morphology, it should have potential applications for being used in biological applications [100]. Similar to α-ZrP, one of the most important aspects to consider for this inorganic laminar nanomaterial in biological applications lies in its ability to provide a controlled release of drugs or charged nanoparticles, while its non-spherical morphology favors its adherence and margination to biological tissue [101,102]. Therefore, just like α-ZrP, α-TiP could be an interesting alternative for drug delivery and bone cement applications, especially if it is enriched with biofunctional nanoparticles that could improve its antimicrobial properties [103,104]. In this context, Adawy et al. recently used the hydrothermal methodology to synthesize monohydrated nanolayered α-TiP, whose surfaces were, afterwards, enriched with AgNPs of uniform dimensions and distribution [65]. After the structural evaluation of the resultant Ag-enriched α-TiP phase, assessments of the cyto-viability and antimicrobial efficacy were performed. Surprisingly, it was reported that α-TiP bears an outstanding cytocompatibility that even surpasses that of α-ZrP, particularly after being enriched with AgNPs [65]. More interestingly, α-TiP appeared to possess higher intercalation capacity for silver ions compared to that of α-ZrP, while, as predicted, AgNPs-enriched α-TiP possessed a perfect

antimicrobial activity [65]. Therefore, these recent results highlight the potential capabilities of α-TiP, especially under stressful biological conditions, in which the decrease in pH values can stimulate more release of the functional silver ions that are richly intercalated in the interlayers of α-TiP.

On the other hand, nanostructured inorganic compounds, such as nanofibrous ρ-TiP and π-TiP, have generated increasing interest in the research directed towards the synthesis of biomaterials. These compounds are usually prepared in advance and used as bone cement or applied as a surface layer covering the implant [105–109], although it is also possible to induce its growth on the substrate surface [110–112]. In the latter case, the thin layer that constitutes the coating acts as a messenger through which interaction with the surrounding biological system occurs [113–115]. The outer layer of the device should be compromised of compounds naturally present in the biological environment, commonly calcium phosphate phases [116–119]. However, nanostructured systems are also used for this application using the metal of the (metallic) substrate as the source of the inorganic matter [120,121]. A good example of these metals is titanium, with high osseointegration capacity and ease of physical attachment to bone, owing to the spontaneously formed oxide layer on its surface, which does not cause denaturation of proteins in the proximity of the implant [122]. Thus, the formation of coating layers of nanostructured compounds containing titanium on the metallic surface of titanium has been described with positive results [123,124], including its use, together with its widely used alloy, titanium–aluminum–vanadium alloy (Ti–6Al–4V), in implant applications [125,126]. Modifications of the surfaces of titanium and its alloys by coating them with a layer of nanostructured materials could promote their hydrophilicity, surface roughness, biocompatibility, and bioactivity, by improving both their functionality and their osseointegration and, therefore, their long-term fixation of the implant. In this respect, the two polymorphs π- and ρ-TiP are nanostructured compounds that obviously contain titanium, the former of which could be grown successfully on titanium surfaces [73–75].

Recently, Adawy et al. synthesized nanorods of the polymorphs π-TiP and ρ-TiP and enriched them with AgNPs that provided outstanding antimicrobial activity without much of a compromise to their cytocompatibility [127]. Additionally, they hydrothermally treated the commercially available Ti–6Al–4V alloy in aqueous phosphoric acid solution in attempts that led to the growth of a nanofibrous coating layer of π-TiP on the surface of Ti–6Al–4V alloy discs, where the size as well as the surface roughness of this nanofibrous π-TiP coating layer can be controlled [127]. Although intercalation is not an option for the nanofibrous morphology of π-TiP, Adawy et al. reported the enrichment of the coated surfaces with AgNPs and their subsequent doping with strontium ions, which in turn played an outstanding role in controlling the release of the antimicrobial AgNPs, in a mechanism that improved the cytocompatibility and long-term biofunctionality of the resultant coated biomedical alloy as they described in their long-term ion release assessments [127].

4. Conclusions

More than half a century of research on metal phosphates has provided multiple synthetic approaches for α-ZrP, some of which were later adopted for the synthesis of α-TiP. The different available synthetic routes allowed for controlling the crystallinity, particle size, textural properties, functionalization and, consequently, the reactivity of these materials. In addition to the traditional methods, based on the use of zirconium (IV) complexing agents, such as fluoride and oxalate, new routes were developed, mainly aimed at obtaining particles with varied morphologies, such as nanoplates, nanofibers, and mesoporous compounds. The research also offered several methods for the effective functionalization of the α-ZrP layers, and thus obtaining tailored materials for specific applications, many of them targeted, among many profound technological applications, in the field of biomedicine research. Although α-ZrP has attracted substantial research attention for biomedical application, mainly in drug delivery applications, α-TiP, as an iso-structure of α-ZrP, has been scarcely investigated in this regard until recently. α-TiP, which shares with its zirconium counterpart many of

the technological applications, could also be the basis for many prospective medicinal applications, particularly after the recent reports on its better biocompatibility compared to α-ZrP. On the other hand, nanofibrous TiP, which has attracted research interests in the latest decade, could also be useful for many prospective technological applications. In addition, it can be considered as an easily functionalized nanostructured material for use in biocement applications, as well as coating for biomedical alloys, thus enhancing their bio-functionality and, ultimately, their long-term success.

Author Contributions: Conceptualization, Z.A. and A.A.; writing—original draft preparation, J.R.G., A.A. and Z.A.; writing—review and editing, A.A.; visualization, A.A.; supervision, A.A.; project administration, Z.A.; funding acquisition, J.R.G. All authors have read and agreed to the published version of the manuscript.

Funding: This review project was funded by MINECO, grant numbers MAT2016-78155-C2-1-R and MCI-415 21-PID2020-113558RB-C41; and by the Government of the Principality of Asturias, grant number 416 GRUPIN-IDI/2018/170.

Acknowledgments: A.A. is genuinely grateful to N.M.K. Nassar for her incredible encouragement and endless support, and dedicates her work in this review to the soul of Adawy M. Hassan, to whom she is eternally grateful.

Conflicts of Interest: The authors declare no conflict of interest.

References

1. Pica, M.; Donnadio, A.; Casciola, M. From microcrystalline to nanosized α zirconium phosphate: Synthetic approaches and applications of an old material with a bright future. *Coord. Chem. Rev.* **2018**, *374*, 218–235. [CrossRef]
2. Kraus, K.A.; Phillips, H.O. Adsorption on inorganic materials. I. Cation exchange properties of zirconium phosphate. *J. Am. Chem. Soc.* **1956**, *78*, 694. [CrossRef]
3. Amphlett, C.B.; McDonald, L.A.; Redman, M.J. Synthetic inorganic ion-exchange materials—I. Zirconium phosphate. *J. Inorg. Nucl. Chem.* **1958**, *6*, 220–235. [CrossRef]
4. Amphlett, C.B.; McDonald, L.A.; Burgess, J.S.; Maynard, J.C. Synthetic inorganic ion-exchange materials—III. The separation of rubidium and cesium on zirconium phosphate. *J. Inorg. Nucl. Chem.* **1959**, *10*, 69–73. [CrossRef]
5. Curtman, L.J.; Greenslade, T.B. Removal of phosphate ion. *J. Chem. Educ.* **1936**, *13*, 238–239. [CrossRef]
6. Holness, H.; Mattock, G. Phosphate removal in qualitative analysis. *Analyst* **1949**, *74*, 43–46. [CrossRef]
7. Friend, J.N.; Vallance, R.H.; Challis, H.J.G. Phosphate separation in qualitative analysis. *Nature* **1940**, *146*, 63. [CrossRef]
8. Kiefer, E.W.; Boltz, D.F. Spectrophotometric determination of zirconium. *Anal. Chem.* **1952**, *24*, 542–544. [CrossRef]
9. Clearfield, A.; Stynes, J.A. The preparation of crystalline zirconium phosphate and some observations on its ion exchange behaviour. *J. Inorg. Nucl. Chem.* **1964**, *26*, 117–129. [CrossRef]
10. Clearfield, A.; Smith, S.D. The crystal structure of zirconium phosphate and the mechanism of its ion exchange behaviour. *J. Colloid Interface Sci.* **1968**, *28*, 325–330. [CrossRef]
11. Clearfield, A.; Smith, G.D. Crystallography and structure of α-zirconium bis(monohydrogenorthophosphate) monohydrate. *Inorg. Chem.* **1969**, *8*, 431–436. [CrossRef]
12. Troup, J.M.; Clearfield, A. Mechanism of ion exchange in zirconium phosphates. 20. Refinement of the crystal structure of α-zirconium phosphate. *Inorg. Chem.* **1977**, *16*, 3311–3314. [CrossRef]
13. Albertsson, J.; Oskarsson, A.; Tellgren, R.; Thomas, J.O. Inorganic ion exchangers. 10. A neutron powder diffraction study of the hydrogen bond geometry in α-zirconium bis(monohydrogenorthophosphate) monohydrate. A model for the ion exchange. *J. Phys. Chem.* **1977**, *81*, 1574–1578. [CrossRef]
14. Pica, M. Zirconium phosphate catalysts in the XXI century: State of the art from 2010 to date. *Catalysts* **2017**, *7*, 190. [CrossRef]
15. Trobajo, C.; Khainakov, S.A.; Espina, A.; García, J.R. On the synthesis of α-zirconium phosphate. *Chem. Mater.* **2000**, *12*, 1787–1790. [CrossRef]
16. Alberti, G.; Torracca, E. Crystalline insoluble salts of polybasic metals—II. Synthesis of crystalline zirconium or titanium phosphate by direct precipitation. *J. Inorg. Nucl. Chem.* **1968**, *30*, 317–318. [CrossRef]
17. García-Rosales, G.; Ordóñez-Regil, E.; Romero-Guzmán, E.T.; Ordóñez-Regil, E. The influence of agitation speed on the morphology and size particle synthesis of $Zr(HPO_4)_2{\cdot}H_2O$ from mexican sand. *J. Mineral. Mater. Charact. Eng.* **2007**, *6*, 39–51.
18. Horsley, S.E.; Nowell, D.V. The preparation and characterization of crystalline α-zirconium phosphate. *J. Appl. Chem. Biotechnol.* **1973**, *23*, 215–224. [CrossRef]
19. Capitani, D.; Casciola, M.; Donnadio, A.; Vivani, R. High yield precipitation of crystalline α-zirconium phosphate from oxalic acid solutions. *Inorg. Chem.* **2010**, *49*, 9409–9415. [CrossRef]
20. Shuai, M.; Mejia, A.F.; Chang, Y.W.; Cheng, Z. Hydrothermal synthesis of layered zirconium phosphate disks: Control of aspect ratio and polydispersity for nano-architecture. *Cryst. Eng. Comm.* **2013**, *15*, 1970–1977. [CrossRef]

21. Vekilov, P.G. Two-step mechanism for the nucleation of crystals from solution. *J. Cryst. Growth* **2005**, *275*, 65–76. [CrossRef]
22. Adawy, A. The Ceiling Method for the Growth of High-Resolution Protein Crystals. Ph.D. Thesis, Radboud University, Nijmegen, The Netherlands, 2014.
23. Adawy, A.; Amghouz, Z.; van Hest, J.C.M.; Daniela, A.W. Sub-micron polymeric stomatocytes as promising templates for confined crystallization and diffraction experiments. *Small* **2017**, *13*, 1700642. [CrossRef] [PubMed]
24. Liu, X.; Chee, S.W.; Raj, S.; Sawczyk, M.; Král, P.; Mirsaidov, U. Three-step nucleation of metal–organic framework nanocrystals. *Proc. Nat. Acad. Sci. USA* **2021**, *118*, e2008880118. [CrossRef] [PubMed]
25. Cheng, Y.; Wang, X.; Jaenicke, S.; Chuah, G.K. Minimalistic liquid assisted route to highly crystalline α-zirconium phosphate. *Chem. Sus. Chem.* **2017**, *10*, 3235–3242. [CrossRef]
26. Benhamza, H.; Barboux, P.; Bouhaouss, A.; Josien, F.A.; Livage, J. Sol–gel synthesis of $Zr(HPO_4)_2{\cdot}H_2O$. *J. Mater. Chem.* **1991**, *1*, 681–684. [CrossRef]
27. Hajipour, A.R.; Karimi, H. Synthesis and characterization of hexagonal zirconium phosphate nanoparticles. *Mater. Lett.* **2014**, *116*, 356–358. [CrossRef]
28. Alberti, G.; Casciola, M.; Marmottini, F.; Vivani, R. Preparation of mesoporous zirconium phosphate-pyrophosphate with a large amount of thermally stable acid groups on the pore surface. *J. Porous Mater.* **1999**, *6*, 299305. [CrossRef]
29. Alberti, G.; Casciola, M.; Cavalaglio, S.; Vivani, R. Proton conductivity of mesoporous zirconium phosphate pyrophosphate. *Solid State Ion.* **1999**, *125*, 91–97. [CrossRef]
30. Clearfield, A.; Thakur, D.S. Zirconium and titanium phosphates as catalysts: A review. *Appl. Catal.* **1986**, *26*, 1–26. [CrossRef]
31. Jiménez-Jiménez, J.; Maireles-Torres, P.; Olivera-Pastor, P.; Rodríguez-Castellón, E.; Jiménez-López, A.; Jones, D.J.; Roziere, J. Surfactant-assisted synthesis of a mesoporous form of zirconium phosphate with acidic properties. *Adv. Mater.* **1998**, *10*, 812–815. [CrossRef]
32. Zhang, F.; Xie, Y.; Lu, W.; Wang, X.; Xu, S.; Lei, X. Preparation of microspherical α-zirconium phosphate catalysts for conversion of fatty acid methyl esters to monoethanolamides. *J. Colloid Interface Sci.* **2010**, *349*, 571–577. [CrossRef] [PubMed]
33. Sinhamahapatra, A.; Sutradhar, N.; Roy, B.; Tarafdar, A.; Bajaj, H.C.; Panda, A.B. Mesoporous zirconium phosphate catalyzed reactions: Synthesis of industrially important chemicals in solvent-free conditions. *Appl. Catal. A* **2010**, *385*, 22–30. [CrossRef]
34. Zhao, G.L.; Yuan, Z.Y.; Chen, T.H. Synthesis of amorphous supermicroporous zirconium phosphate materials by nonionic surfactant templating. *Mater. Res. Bull.* **2005**, *40*, 1922–1928. [CrossRef]
35. Tarafdar, A.; Panda, A.B.; Pradhan, N.C.; Pramanik, P. Synthesis of spherical mesostructured zirconium phosphate with acidic properties. *Microporous Mesoporous Mater.* **2006**, *95*, 360–365. [CrossRef]
36. Zhu, Y.; Shimizu, T.; Kitajima, T.; Morisato, K.; Moitra, N.; Brun, N.; Kiyomura, T.; Kanamori, K.; Takeda, K.; Kurata, H.; et al. Synthesis of robust hierarchically porous zirconium phosphate monolith for efficient ion adsorption. *New J. Chem.* **2015**, *39*, 2444–2450. [CrossRef]
37. Bellezza, F.; Cipiciani, A.; Costantino, U.; Marmottini, F.; Quotadamo, M.A. Zirconium phosphate nanoparticles from water-in-oil microemulsions. *Colloid Polym. Sci.* **2006**, *285*, 19–25. [CrossRef]
38. Alberti, G.; Casciola, M.; Capitani, D.; Donnadio, A.; Narducci, R.; Pica, M.; Sganappa, M. Novel Nafion–zirconium phosphate nanocomposite membranes with enhanced stability of proton conductivity at medium temperature and high relative humidity. *Electrochim. Acta* **2007**, *52*, 8125–8132. [CrossRef]
39. Gescher, A. Metabolism of N,N-dimethylformamide: Key to the understanding of its toxicity. *Chem. Res. Toxicol.* **1993**, *6*, 245–251. [CrossRef]
40. Pica, M.; Donnadio, A.; Capitani, D.; Vivani, R.; Troni, E.; Casciola, M. Advances in the chemistry of nanosized zirconium phosphates: A new mild and quick route to the synthesis of nanocrystals. *Inorg. Chem.* **2011**, *50*, 11623–11630. [CrossRef]
41. Li, Z.; Vivas, E.L.; Suh, Y.J.; Cho, K. Highly efficient and selective removal of Sr^{2+} from aqueous solutions using ammoniated zirconium phosphate. *J. Environ. Chem. Eng.* **2022**, *10*, 107333. [CrossRef]
42. Pan, S.; Shen, J.; Deng, Z.; Zhang, X.; Pan, B. Metastable nano-zirconium phosphate inside gel-type ion exchanger for enhanced removal of heavy metals. *J. Hazard. Mater.* **2022**, *423*, 127158. [CrossRef] [PubMed]
43. Bashir, A.; Ahad, S.; Malik, L.A.; Qureashi, A.; Manzoor, T.; Dar, G.N.; Pandith, A.H. Revisiting the old and golden inorganic material, zirconium phosphate: Synthesis, intercalation, surface functionalization, and metal ion uptake. *Ind. Eng. Chem. Res.* **2020**, *59*, 22353–22397. [CrossRef]
44. Colodrero, R.M.P.; Olivera-Pastor, P.; Cabeza, A.; Bazaga-García, M. Properties and Applications of Metal Phosphates and Pyrophosphates as Proton Conductors. *Materials* **2022**, *15*, 1292. [CrossRef] [PubMed]
45. Zhao, Y.; Yan, S.; He, Y.; Li, Z.; Li, C.; Li, H. Synthesis of ultrathin α-zirconium phosphate functionalized with polypyrrole for reinforcing the anticorrosive property of waterborne epoxy coating. *Colloids Surf. A Physicochem. Eng. Asp.* **2022**, *635*, 128052. [CrossRef]
46. Zhao, M.; Baker, J.; Jiang, Z.; Zhu, Z.; Wu, H.-M.; Wu, J.-L.; Kang, W.-H.; Sue, H.-J. Preparation of Well-Exfoliated Poly(ethylene-co-vinyl acetate)/alpha-Zirconium Phosphate Nanocomposites. *Langmuir* **2021**, *37*, 4550–4561. [CrossRef]
47. Zhu, Z.; Tsai, C.-Y.; Zhao, M.; Baker, J.; Sue, H.-J. PMMA Nanocomposites Based on PMMA-Grafted α-Zirconium Phosphate Nanoplatelets. *Macromolecules* **2022**, *55*, 1165–1177. [CrossRef]
48. Díaz, A.; David, A.; Pérez, R.; González, M.L.; Báez, A.; Wark, S.E.; Zhang, P.; Clearfield, A.; Colón, J.L. Nanoencapsulation of insulin into zirconium phosphate for oral delivery applications. *Biomacromolecules* **2010**, *11*, 2465–2470. [CrossRef]

49. Saxena, V.; Díaz, A.; Clearfield, A.; Batteas, J.D.; Hussain, M.D. Zirconium phosphate nanoplatelets: A biocompatible nanomaterial for drug delivery to cancer. *Nanoscale* **2013**, *5*, 2328–2336. [CrossRef]
50. Díaz, A.; Saxena, V.; González, J.; David, A.; Casanas, B.; Carpenter, C.; Batteas, J.D.; Colón, J.L.; Clearfield, A.; Hussain, M.D. Zirconium phosphate nanoplatelets: A novel platform for drug delivery in cancer therapy. *Chem. Commun.* **2012**, *48*, 1754–1756. [CrossRef]
51. Díaz, A.; González, M.L.; Pérez, R.J.; David, A.; Mukherjee, A.; Báez, A.; Clearfield, A.; Colón, J.L. Direct intercalation of cisplatin into zirconium phosphate nanoplatelets for potential cancer nanotherapy. *Nanoscale* **2013**, *5*, 11456–11463. [CrossRef]
52. Wester, M.; Simonis, F.; Gerritsen, K.G.; Boer, W.H.; Wodzig, W.K.; Kooman, J.P.; Joles, J.A. A regenerable potassium and phosphate sorbent system to enhance dialysis efficacy and device portability: An in vitro study. *Nephrol. Dyalysis Transp.* **2013**, *28*, 2364–2371. [CrossRef] [PubMed]
53. Ding, Y.; Jones, D.J.; Maireles-Torres, P.; Roziere, J. Two dimensional nanocomposites: Alternating inorganic-organic polymer layers in zirconium phosphate. *Chem. Mater.* **1995**, *7*, 562–571. [CrossRef]
54. Kumar, C.; Mclendon, G. Nanoencapsulation of cytochrome c and horseradish peroxidase at the galleries of α-zirconium phosphate. *Chem. Mater.* **1997**, *9*, 863–870. [CrossRef]
55. Kim, H.N.; Keller, S.W.; Mallouk, T.E. Characterization of zirconium phosphate/polycation thin films grown by sequential adsorption reactions. *Chem. Mater.* **1997**, *9*, 1414–1421. [CrossRef]
56. Kumar, C.V.; Chaudhuri, A. Proteins immobilized at the galleries of layered α-zirconium phosphate: Structure and activity studies. *J. Am. Chem. Soc.* **2000**, *122*, 830–837. [CrossRef]
57. Bellezza, F.; Cipiciani, A.; Costantino, U.; Negozio, M.E. Zirconium phosphate and modified zirconium phosphates as supports of lipase. Preparation of the composites and activity of the supported enzyme. *Langmuir* **2002**, *18*, 8737–8742. [CrossRef]
58. Mudhivarthi, V.K.; Bhambhani, A.; Kumar, C.V. Novel enzyme/DNA/inorganic nanomaterials: A new generation of biocatalysts. *Dalton Trans.* **2007**, *36*, 5483–5497. [CrossRef]
59. Bhambhani, A.; Kumar, C.V. Enzyme-inorganic nanoporous materials: Stabilization of proteins intercalated in α-zirconium phosphate by a denaturant. *Micropor. Mesopor. Mater.* **2008**, *110*, 517–527. [CrossRef]
60. Xu, S.; Whitin, J.C.; Yu, T.T.; Zhou, H.; Sun, D.; Sue, H.S.; Zou, H.; Cohen, H.J.; Zare, R.N. Capture of phosphopeptides using α-zirconium phosphate nanoplatelets. *Anal. Chem.* **2008**, *80*, 5542–5549. [CrossRef]
61. González, M.L.; Ortiz, M.; Hernández, C.; Cabán, J.; Rodríguez, A.; Colón, J.L.; Báez, A. Zirconium phosphate nanoplatelet potential for anticancer drug delivery applications. *J. Nanosci. Nanotechnol.* **2016**, *16*, 117–129. [CrossRef]
62. González-Villegas, J.; Kan, Y.; Bakhmutov, V.I.; García-Vargas, A.; Martínez, M.; Clearfield, A.; Colón, J.L. Poly(ethylene glycol)-modified zirconium phosphate nanoplatelets for improved doxorubicin delivery. *Inorg. Chim. Acta* **2017**, *468*, 270–279. [CrossRef]
63. Li, R.; Liu, T.; Wang, K. Hyaluronic acid-modified zirconium phosphate nanoparticles for potential lung cancer therapy. *Biomed. Eng. Biomed. Tech.* **2016**, *62*, 67–73. [CrossRef] [PubMed]
64. Donnadio, A.; Ambrogi, V.; Pietrella, D.; Pica, M.; Sorrentino, G.; Casciola, M. Carboxymethylcellulose films containing chlorhexidine–zirconium phosphate nanoparticles: Antibiofilm activity and cytotoxicity. *RSC Adv.* **2016**, *6*, 46249. [CrossRef]
65. García, I.; Trobajo, C.; Amghouz, Z.; Adawy, A. Nanolayered metal phosphates as biocompatible reservoirs for antimicrobial silver nanoparticles. *Materials* **2021**, *14*, 1481. [CrossRef]
66. Alberti, G.; Cardini-Galli, P.; Costantino, U.; Torracca, E. Crystalline insoluble salts of polybasic metals. 1. Ion-exchange properties of crystalline titanium phosphate. *J. Inorg. Nucl. Chem.* **1967**, *29*, 571–578. [CrossRef]
67. Chernorukov, N.G.; Moskvich, E.P.; Zhuk, M.I. Crystallographic characteristics of phosphates and arsenates of tetravalent elements. *Kristallograf.* **1974**, *19*, 1084–1085.
68. Suárez, M.; García, J.R.; Rodríguez, J. Calorimetric determination of H^+/Na^+ ion-exchange on α-titanium phosphate. *J. Phys. Chem.* **1984**, *88*, 157–159. [CrossRef]
69. Suárez, M.; García, J.R.; Rodríguez, J. Thermodynamic treatment of H^+/Na^+ ion-exchange on α-titanium phosphate. *J. Phys. Chem.* **1984**, *88*, 159–162. [CrossRef]
70. García, J.R.; Suárez, M.; Guarido, C.G.; Rodríguez, J. X-Ray diffraction spectrometry for the analysis of crystalline solid phases. *Anal. Chem.* **1984**, *56*, 193–196. [CrossRef]
71. Kumada, N.; Imase, A.; Yanagida, S.; Takei, T.; Miura, A.; Itoi, N.; Goto, T. Hydrothermal synthesis of $KTi_2(PO_4)_3$, α-$Ti(HPO_4)_2{\cdot}H_2O$ and γ-Ti $(PO_4)(H_2PO_4){\cdot}2H_2O$ from a lepidocrocite-type titanate. *J. Asian Ceram. Soc.* **2019**, *7*, 361–367. [CrossRef]
72. Bortun, A.I.; Khainakov, S.A.; Bortun, L.N.; Poojary, D.M.; Rodriguez, J.; Garcia, J.R.; Clearfield, A. Synthesis and Characterization of Two Novel Fibrous Titanium Phosphates $Ti_2O(PO_4)_2{\cdot}2H_2O$. *Chem. Mater.* **1997**, *9*, 1805–1811. [CrossRef]
73. Park, J.-W.; Jang, J.-H.; Lee, C.S.; Hanawa, T. Osteoconductivity of hydrophilic microstructured titanium implants with phosphate ion chemistry. *Acta Biomater.* **2009**, *5*, 2311–2321. [CrossRef] [PubMed]
74. Lu, J.-S. Corrosion of titanium in phosphoric acid at 250 °C. *Trans. Nonferrous Met. Soc. China* **2009**, *19*, 552–556. [CrossRef]
75. Yada, M.; Inoue, Y.; Sakamoto, A.; Torikai, T.; Watari, T. Synthesis and controllable wettability of micro-and nanostructured titanium phosphate thin films formed on titanium plates. *ACS Appl. Mater. Interfaces* **2014**, *6*, 7695–7704. [CrossRef] [PubMed]
76. Salvadó, M.A.; Pertierra, P.; García-Granda, S.; García, J.R.; Rodríguez, J. Fernández-Díaz, M.T. Neutron powder diffraction study of α-$Ti(HPO_4)_2{\cdot}H_2O$ and α-$Hf(HPO_4)_2{\cdot}H_2O$.; H-atom positions. *Acta Cryst. B* **1996**, *52*, 896–898. [CrossRef]

77. Christensen, A.N.; Andersen, E.K.; Andersen, I.G.K.; Alberti, G.; Nielsen, M.; Lehmann, M.S. X-Ray powder diffraction study of layer compounds. The crystal structure of alpha-Ti(HPO_4)$_2$·H_2O and a proposed structure for gamma-Ti(H_2PO_4)(PO_4)·2H_2O. *Acta. Chem. Scand.* **1990**, *44*, 865–872. [CrossRef]
78. Poojary, D.M.; Shpeizer, B.; Clearfield, A. X-Ray powder structure and Rietveld refinement of γ-zirconium phosphate, Zr(PO_4)(H_2PO_4)·2H_2O. *J. Chem. Soc. Dalton Trans.* **1995**, *19*, 111–113. [CrossRef]
79. Krogh Andersen, A.M.; Norby, P.; Vogt, T. Determination of formation regions of titanium phosphates; determination of the crystal structure of β-titanium phosphate, Ti(PO_4)(H_2PO_4), from neutron powder data. *J. Solid State Chem.* **1998**, *140*, 266–271. [CrossRef]
80. Llavona, R.; Suárez, M.; García, J.R.; Rodríguez, J. Lamellar inorganic ion exchangers. Alkali metal ion exchange on α- and γ-titanium phosphate. *Inorg. Chem.* **1989**, *28*, 2863–2868. [CrossRef]
81. Zhou, G.F.; Wang, Q.; Zeng, R.Q.; Fu, X.K.; Yang, X.B. Preparation and application of zirconium phosphate and its derivatives. *Progress Chem.* **2014**, *26*, 87–99.
82. Kishore, M.S.; Pralong, V.; Caignaert, V.; Varadaraju, U.V.; Raveau, B. Electrochemical intercalation of lithium in the titanium hydrogeno phosphate Ti(HPO_4)$_2$·H_2O. *J. Power Sources* **2007**, *169*, 355–360. [CrossRef]
83. Lee, G.; Zhang, X.; Zhang, H.B.; Varanasi, C.V.; Liu, J. Effect of interlayer spacing on sodium ion insertion in nanostructured titanium hydrogeno phosphates/carbon nanotube composite. *RSC Adv.* **2016**, *6*, 60015–60021. [CrossRef]
84. Xiang, X.; Li, X.; Chen, K.; Tang, Y.; Wan, M.; Ding, X.; Xue, L.; Zhang, W.; Huang, Y. Gamma titanium phosphate as an electrode material for Li-ion and Na-ion storage: Performance and mechanism. *J. Mater. Chem. A* **2016**, *4*, 18084–18090. [CrossRef]
85. García-Glez, J.; Trobajo, C.; Khainakov, S.A.; Amghouz, Z. α-Titanium phosphate intercalated with propylamine: An alternative pathway for efficient europium (III) uptake into layered tetravalent metal phosphates. *Arab. J. Chem.* **2017**, *10*, 885–894. [CrossRef]
86. García-Glez, J.; Trobajo, C.; Adawy, A.; Amghouz, Z. Exfoliation and europium (III)-functionalization of α-titanium phosphate via propylamine intercalation: From multilayer assemblies to single nanosheets. *Adsorption* **2020**, *26*, 241–250. [CrossRef]
87. Albitres, G.A.V.; Cestari, S.P.; Freitas, D.F.S.; Rodrigues, D.C.; Mendes, L.C.; Neumann, R. Intercalation of α-titanium phosphate with longchain amine aided by short-chain amine. *Appl. Nanosci.* **2020**, *10*, 907–916. [CrossRef]
88. Bortun, A.I.; Bortun, L.N.; Clearfied, A.; Villa-García, M.A.; García, J.R.; Rodríguez, J. Synthesis and characterization of a novel layered titanium phosphate. *J. Mater. Res.* **1996**, *11*, 2490–2498. [CrossRef]
89. García-Granda, S.; Salvadó, M.A.; Pertierra, P.; Bortun, A.I.; Khainakov, S.A.; Trobajo, C.; Espina, A.; García, J.R. Hydrothermal synthesis and characterization of an ammoniumtitanium (IV) phosphate with pyrochlore-type structure. *Inorg. Chem. Comm.* **2001**, *4*, 555–557. [CrossRef]
90. Blanco, J.A.; Khainakov, S.A.; Khainakova, O.; García, J.R.; García-Granda, S. An old material in the nanoworld: Organic-inorganic hybrid nanotubes based on γ-titanium phosphate layered crystal structure. *Phys. Status Solidi C* **2009**, *6*, 2190–2194. [CrossRef]
91. García-Granda, S.; Khainakov, S.A.; Espina, A.; García, J.R.; Castro, G.R.; Rocha, J.; Mafra, L. Revisiting the thermal decomposition of layered γ-titanium phosphate and structural elucidation of its intermediate phases. *Inorg. Chem.* **2010**, *49*, 2630–2638. [CrossRef]
92. Espina, A.; Trobajo, C.; Khainakov, S.A.; García, J.R.; Salvadó, M.A.; Pertierra, P.; García-Granda, S. Reaction of π-$Ti_2O(PO_4)_2$·2H_2O with molten alkali nitrates. Synthesis of the fibrous materials π-$M_{0.5}H_{0.5}TiOPO_4$ (M = Na, K). *Mater. Res. Bull.* **2002**, *37*, 1381–1392. [CrossRef]
93. Espina, A.; Trobajo, C.; Khainakov, S.A.; García, J.R. Synthesis of the fibrous materials ρ-$Na_{0.50}H_{0.50}TiOPO_4$ and ρ-$K_{0.67}H_{0.33}TiOPO_4$ by reaction of ρ-$Ti_2O(PO_4)_2(H_2O)_2$ with molten alkali nitrates. *Mater. Res. Bull.* **2001**, *36*, 2531–2541. [CrossRef]
94. Salvadó, M.A.; Pertierra, P.; García-Granda, S.; García, J.R.; Fernández- Díaz, M.T.; Dooryhee, E. Crystal structure, including H-atom positions, of $Ti_2O(PO_4)_2(H_2O)_2$ determined from synchrotron X-ray and neutron powder data. *Eur. J. Solid State Inorg. Chem.* **1997**, *34*, 1237–1247. [CrossRef]
95. Babaryk, A.A.; Adawy, A.; García, I.; Trobajo, C.; Amghouz, Z.; Colodrero, R.M.P.; Cabeza, A.; Olivera-Pastor, P.; Bazaga-García, M.; dos Santos-Gómez, L. Structural and proton conductivity studies of fibrous π-$Ti_2O(PO_4)_2$·2H_2O: Application in chitosan-based composite membranes. *Dalton Trans.* **2021**, *50*, 7667–7677. [CrossRef]
96. Bereznitski, Y.; Jaroniec, M.; Bortun, A.I.; Poojary, D.M.; Clearfield, A. Surface and structural properties of novel titanium phosphates. *J. Colloid Interface Sci.* **1997**, *191*, 442–448. [CrossRef]
97. García-Glez, J.; Amghouz, Z.; da Silva, I.; Ania, C.O.; Parra, J.B.; Trobajo, C.; García-Granda, S. The ability of a fibrous titanium oxophosphate for nitrogen-adsorption above room temperature. *Chem. Commun.* **2017**, *53*, 2249–2251. [CrossRef]
98. Cai, B.; Jiang, N.; Tan, P.; Hou, Y.; Li, Y.B.; Zhang, L. The custom making of hierarchical micro/nanoscaled titanium phosphate coatings and their formation mechanism analysis. *RSC Adv.* **2019**, *9*, 41311–41318. [CrossRef]
99. Prabakar, S.J.R.; Park, W.-B.; Seo, J.Y.; Singh, S.P.; Ahn, D.; Sohn, K.-S.; Pyo, M. Ultra-stable $Ti_2O(PO_4)_2(H_2O)$ as a viable new Ca^{2+} storage electrode material for calcium-ion batteries. *Energy Storage Mater.* **2021**, *43*, 85–96. [CrossRef]
100. Korneikov, R.I.; Aksenova, S.V.; Ivanenko, V.I.; Lokshin, E.P. Stability of titanyl hydrogen phosphates in aqueous media. *Inorg. Mater.* **2018**, *54*, 689–693. [CrossRef]
101. Geng, Y.; Dalhaimer, P.; Cai, S.; Tsai, R.; Tewari, M.; Minko, T.; Discheret, D.E. Shape effects of filaments versus spherical particles in flow and drug delivery. *Nat. Nanotech.* **2007**, *2*, 249–255. [CrossRef]
102. Decuzzi, P.; Ferrari, M. The receptor-mediated endocytosis of nonspherical particles. *Biophy. J.* **2008**, *94*, 3790–3797. [CrossRef]
103. Prabhu, S.; Poulose, E.K. Silver nanoparticles: Mechanism of antimicrobial action, synthesis, medical applications, and toxicity effects. *Int. Nano Lett.* **2012**, *2*, 32. [CrossRef]

104. Wypij, M.; Jędrzejewski, T.; Ostrowski, M.; Trzcińska, J.; Rai, M.; Golińska, P. Biogenic silver nanoparticles: Assessment of their cytotoxicity, genotoxicity and study of capping proteins. *Molecules* **2020**, *25*, 3022. [CrossRef] [PubMed]
105. Roşu, R.A.; Şerban, V.A.; Bucur, A.I.; Dragoş, U. Deposition of titanium nitride and hydroxyapatite-based biocompatible composite by reactive plasma spraying. *App. Surf. Sci.* **2011**, *258*, 3871–3876. [CrossRef]
106. Esteban-Tejeda, L.; Díaz, L.A.; Cabal, B.; Prado, C.; López-Piriz, R.; Torrecillas, R.; Moya, J.S. Biocide glass–ceramic coating on titanium alloy and zirconium oxide for dental applications. *Mater. Lett.* **2013**, *111*, 59–62. [CrossRef]
107. Mondal, J.; Aarik, L.; Kozlova, J.; Niilisk, A.; Mändar, H.; Mäeorg, U.; Simões, A.; Sammelselg, V. Functionalization of Titanium Alloy Surface by Graphene Nanoplatelets and Metal Oxides: Corrosion Inhibition. *J. Nanosci. Nanotechnol.* **2015**, *15*, 6533–6540. [CrossRef]
108. Castellini, I.; Andreani, L.; Parchi, P.D.; Bonicoli, E.; Piolanti, N.; Risoli, F.; Lisanti, M. Hydroxyapatite in total hip arthroplasty. Our experience with a plasma spray porous titanium alloy/hydroxyapatite double-coated cementless stem. *Clin. Cases Miner. Bone Metab.* **2016**, *13*, 221–227. [CrossRef]
109. Li, K.; Yan, J.; Wang, C.; Bi, L.; Zhang, Q.; Han, Y. Graphene modified titanium alloy promote the adhesion, proliferation and osteogenic differentiation of bone marrow stromal cells. *Biochem. Biophys. Res. Comm.* **2017**, *489*, 187–192. [CrossRef]
110. Gnedenkov, S.V.; Sinebryukhov, S.L.; Puz, A.V.; Egorkin, V.S.; Kostiv, R.E. In vivo study of osteogenerating properties of calciumphosphate coating on titanium alloy Ti-6Al-4V. *Biomed. Mater. Eng.* **2016**, *27*, 551–560.
111. Trybuś, B.; Zieliński, A.; Beutner, R.; Seramak, T.; Scharnweber, D. Deposition of phosphate coatings on titanium within scaffold structure. *Acta Bioeng. Biomech.* **2017**, *19*, 65–72.
112. Chellappa, M.; Vijayalakshmi, U. Electrophoretic deposition of silica and its composite coatings on Ti-6Al-4V, and its in vitro corrosion behaviour for biomedical applications. *Mater. Sci. Eng. C Mater. Biol. Appl.* **2017**, *71*, 879–890. [CrossRef] [PubMed]
113. Meyer, U.; Joos, U.; Mythili, J.; Stamm, T.; Hohoff, A.; Fillies, T.; Stratmann, U.; Wiesmann, H.P. Ultrastructural characterization of the implant/bone interface of immediately loaded dental implants. *Biomaterials* **2004**, *25*, 1959–1967. [CrossRef] [PubMed]
114. Sharan, J.; Koul, V.; Dinda, A.K.; Kharbanda, O.P.; Lale, S.V.; Duggal, R.; Mishra, M.; Gupta, G.; Singh, M.P. Bio-functionalization of grade V titanium alloy with type I human collagen for enhancing and promoting human periodontal fibroblast cell adhesion: An in-vitro study. *Colloids Surf. B Biointerface* **2018**, *161*, 1–9. [CrossRef] [PubMed]
115. AlFarraj, A.A.; Sukumaran, A.; Al Amri, M.D.; Van Oirschot, A.B.; Jansen, J.A. A comparative study of the bone contact to zirconium and titanium implants after 8 weeks of implantation in rabbit femoral condyles. *Odontology* **2018**, *106*, 37–44. [CrossRef]
116. Hassan, A.A.M. Surface Modification and Biophysical Characterization of a Prosthetic Alloy. Master's Thesis, Ain Shams University, Cairo, Egypt, 2008.
117. Adawy, A.; Abdel-Fattah, W.I.; Talaat, M.S.; El-Sayed, M.E.-S. Biomimetic coating of a precalcified Ti-6Al-4V alloy. *Open Med. Devices* **2009**, *1*, 19–28. [CrossRef]
118. Abdel-Fattah, W.I.; El-Sayed, M.E.-S.; Talaat, M.S.; Adawy, A. Comparative Study of Sr^{2+} and Zn^{2+} incorporation in the biomimetic coating of a prosthetic alloy. *Open Biomater. J.* **2011**, *3*, 4–13. [CrossRef]
119. Adawy, A.; Abdel-Fattah, W.I. An efficient biomimetic coating methodology for a prosthetic alloy. *Mater. Sci. Eng. C Mater. Biolog. App.* **2013**, *33*, 1813–1818. [CrossRef]
120. Jiang, N.; Guo, Z.; Sun, D.; Li, Y.; Yang, Y.; Chen, C.; Zhang, L.; Zhu, S. Promoting osseointegration of Ti implants through micro/nanoscaled hierarchical Ti phosphate/Ti oxide hybrid coating. *ACS Nano* **2018**, *12*, 7883–7891. [CrossRef]
121. Leelanarathiwat, K.; Minato, K.; Katsuta, Y.; Otsuka, Y.; Katsuragi, H.; Watanabe, F. Cytotoxicity of hydroxyapatite-tyrosine complex with gray titania coating on titanium alloy surface to L929 mouse fibroblasts. *Dent. Mater. J.* **2019**, *38*, 573–578. [CrossRef]
122. Raines, A.L.; Olivares-Navarrete, R.; Wieland, M.; Cochran, D.L.; Schwartz, Z.; Boyan, B.D. Regulation of angiogenesis during osseointegration by titanium surface microstructure and energy. *Biomaterials* **2010**, *31*, 4909–4917. [CrossRef]
123. Tschernitschek, H.; Borchers, L.; Geurtsen, W. Non alloyed titanium as a bioinert metal: A review. *Quintessence Int.* **2005**, *36*, 523–530. [PubMed]
124. Yada, M.; Inoue, Y.; Akihito, G.; Noda, I.; Torikai, T.; Watari, T.; Hotokebuchi, T. Apatite-forming ability of titanium compound nanotube thin films formed on a titanium metal plate in a simulated body fluid. *Colloids Surf. B Biointerfaces* **2010**, *80*, 116–124. [CrossRef] [PubMed]
125. Liu, X.; Chu, P.K.; Ding, C. Surface modification of titanium, titanium alloys, and related materials for biomedical applications. *Mater. Sci. Eng. Res.* **2004**, *92*, 49–121. [CrossRef]
126. Gil, F.J.; Manzanares, N.; Badet, A.; Aparicio, C.; Ginebra, M.P. Biomimetic treatment on dental implants for short-term bone regeneration. *Clin. Oral Investig.* **2014**, *18*, 59–66. [CrossRef] [PubMed]
127. García, I.; Trobajo, C.; Amghouz, Z.; Alonso-Guervos, M.; Díaz, R.; Mendoza, R.; Mauvezín-Quevedo, M.; Adawy, A. Ag- and Sr-enriched nanofibrous titanium phosphate phases as potential antimicrobial cement and coating for a biomedical alloy. *Mater. Sci. Eng. C* **2021**, *126*, 112168. [CrossRef] [PubMed]